Turk J Phys
36 (2012) , 415 – 421.

doi:10.3906/fiz-1111-9

Structural and magnetic characterization of $Bi_{0.9}Ca_{0.1}Fe_{0.98}X_{0.02}O_3$ (X = Mg, Al, Ti, V) polycrystalline multiferroic compounds

Mansour AL-HAJ
Physics Department, Mutah University, Mutah-JORDAN
e-mail: mansour@mutah.edu.jo

Received: 27.11.2011

Abstract

The multiferroic compounds $Bi_{0.9}Ca_{0.1}Fe_{0.98}X_{0.02}O_3$, $X = \{$Mg, Al, Ti, V$\}$, were prepared by the solid state reaction method and were characterized by X-ray diffraction, Fourier transform infrared spectroscopy, vibrating sample magnetometry, and differential scanning calorimetry. The compounds were found to have the rhombohedral perovskite-like structure, accompanied by the existence of small amounts of the usual impurity phases $Bi_2Fe_4O_9$ and $Bi_{25}FeO_{40}$. The appearance of weak ferromagnetism is due to partial destruction of the spiral spin structure due to lattice distortion and suppression of oxygen vacancies. The magnetic transition temperatures of the compounds are 342, 346, 349, and 345 °C, respectively.

Key Words: Multiferroics, X-ray diffraction, magnetization, transition temperature

1. Introduction

$BiFeO_3$ (BFO) is a multiferroic material which simultaneously exhibits electric and magnetic ordering, and has a rhombohedrally distorted perovskite structure with space group R3c. It is a G-type canted antiferromagnetic in which the Fe^{3+} magnetic moments are coupled ferromagnetically within the pseudocubic (111) plane and antiferromagnetically between adjacent planes, with a magnetic transition temperature T_N around 370 °C [1]. Also, BFO is ferroelectric above room temperature with a transition temperature $T_C \cong 830$ °C, which makes it a candidate material for numerous multifunctional device applications. However, due to its spatially modulated spiral spin structure, any net magnetization cannot be observed in bulk BFO at room temperature. Besides that, impurity phases and large leakage current density are major drawbacks associated with this material.

Structure modification and improvement of electrical, optical, and magnetic properties of BFO were achieved by minor substitution of Bi^{3+} by rare earth ions [2-10], alkaline earth ions [11], transition-metal ions [12–15], or by simultaneous minor substitution of Bi^{3+} and Fe^{3+} by ions such as (Ca^{2+}, Ti^{4+}) [16] and (Sr^{2+}, Sc^{3+}, Ti^{4+}) [17]. Various methods, besides the conventional one [18], were used for material synthesis in bulk

and nanopowder forms, such as sol-gel [19, 20], solution combustion [21, 22], hydrothermal [23], and rapid liquid phase sintering [24].

The mechanism by which ion substitution affects the electrical, optical, and magnetic properties of BFO is not totally understood, and further research work is still required for a better understanding of this system. For this reason, we report in this article the structural and magnetic properties of the polycrystalline multiferroic compounds $Bi_{0.9}Ca_{0.1}Fe_{0.98}X_{0.02}O_3$, $X = \{Mg, Al, Ti, V\}$. For brevity, we will refer to these compounds as CaMg, CaAl, CaTi, and CaV, respectively. Only 2% Fe^{3+} was replaced by various ions to make sure that these ions will enter the B sites of the rhomohedral lattice.

2. Experimental

The samples were prepared by the conventional ceramic method. Pure oxides of Bi_2O_3, CaO, Al_2O_3, Fe_2O_3, TiO_2, and V_2O_5 were weighed, mixed, and ground in an agate mortar and pestle. The CaMg mixture was calcined at 825 ^oC in a Carbolite tube furnace for 1.5 h. After calcination, the sample was slowly cooled to room temperature, ground, and calcined again at 825 ^oC for 1.5 h. After the second calcination, the sample was ground in order to obtain a powder form. The same procedure was repeated for the CaAl, CaTi, and CaV mixtures, with the first calcination at 800 ^oC for 0.5 h and the second calcination at 830 ^oC for 1.5 h. These are the optimum conditions for good quality samples. The X-ray diffraction (XRD) patterns were recorded using a Seifert 3003 TT diffractometer operating at 40 kV and 40 mA, using CuK_α radiation ($\lambda = 1.5406$ Å). The instrument was calibrated using a standard Si powder. The Fourier transform infrared (FTIR) spectra were recorded by a Mattson 5000 FTIR spectrometer. The magnetic measurements were made on equal mass samples using a 9600 LDJ vibrating sample magnetometer, which was calibrated using a Ni standard. The magnetic transition temperature was measured by a Mettler differential scanning calorimeter, which was calibrated using an In standard.

3. Results and discussion

The XRD patterns of the studied compounds are shown in Figures 1(a–d), and indicate the formation of the rhombohedral perovskite-like BFO structure with no coexistence of any orthorhombic phases. However, the diffraction peaks, marked by the symbols ♦ and •, indicate the existence of small amounts of the impurity phases $Bi_2Fe_4O_9$ and $Bi_{25}FeO_{40}$, respectively. These phases are the usual phases reported to form during the synthesis of some BFO-based compounds [2, 6, 10–12, 21, 25], and could not be removed even by longer calcination times which also would lead to more volatilization of Bi. It is noteworthy that the amount of impurity phases varies from one compound to another, probably due to the different valence states and ionic radii of the substituting ions.

The Miller indices (hkl) of the diffraction peaks in Figure 1 were referred to hexagonal axes rather than rhombohedral axes. The lattice parameters a and c of the hexagonal unit cell were calculated using the same equation that we used in our previous work [18]. The strong peaks (012), (110), (104), (202), (024), and (300) were employed for such calculations. The values of these parameters, in addition to the ratio c/a, are listed in Table 1, and are in good agreement with values reported for other multiferroic compounds [5, 9, 15, 17, 24]. As known, the ratio c/a is an important structural parameter because it is a measure of the distortion in the rhombohedral lattice (more details regarding this matter can be found in [18]).

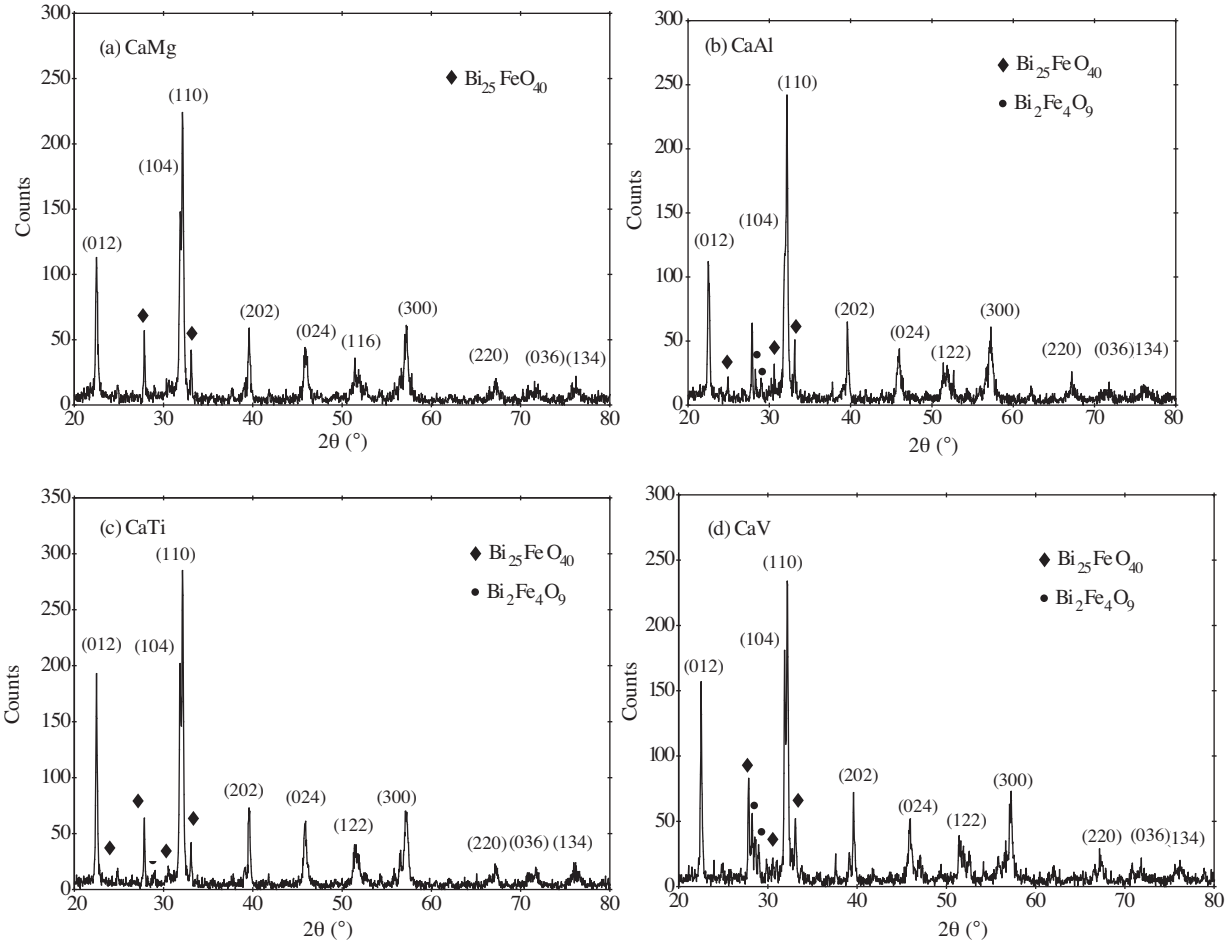

Figure 1. The XRD patterns of (a) $Bi_{0.9}Ca_{0.1}Fe_{0.98}Mg_{0.02}O_3$ (labeled as CaMg), (b) $Bi_{0.9}Ca_{0.1}Fe_{0.98}Al_{0.02}O_3$ (CaAl), (c) $Bi_{0.9}Ca_{0.1}Fe_{0.98}Ti_{0.02}O_3$ (CaTi), and (d) $Bi_{0.9}Ca_{0.1}Fe_{0.98}V_{0.02}O_3$ (CaV).

Table 1. Structural parameters of the studied compounds and the effective radii of the substituting ions.

	a (Å)	c (Å)	c/a	R (Å)
CaMg	5.5672	13.8330	2.4847	0.720
CaAl	5.5656	13.7651	2.4732	0.535
CaTi	5.5660	13.8083	2.4808	0.605
CaV	5.5649	13.7700	2.4744	0.540

In addition to structural parameters, the effective radii of the substituting ions Mg^{2+}, Al^{3+}, Ti^{4+}, and V^{5+} [26] were inserted in Table 1 for comparison purposes. The diversity in the values of c/a for the compounds indicates the difference in the amount of lattice distortion. It is obvious from Table 1 that the c/a value is proportional to the effective ionic radius, as expected, being greatest for CaMg, which means that its crystal lattice is the most distorted one.

Besides XRD, FTIR spectroscopy is particularly important when analyzing multiferroic materials. The FTIR spectra (transmittance T versus wavenumber) of the compounds recorded at room temperature in the

range 500–1000 cm^{-1} are shown in Figure 2. The CaMg spectrum is characterized by a peak at 557 cm^{-1}, while each spectrum of the CaAl, CaTi, and CaV compounds is characterized by a peak at 559 cm^{-1}. These peaks are assigned to the mode of stretching vibrations along the Fe-O axis, being a characteristic of the octahedral FeO_6 units in the perovskite structure. These spectra indicate that our samples are of good quality despite the existence of small impurity phases. The mode characteristic of Fe-O bending vibrations is not seen in our spectra because it lies out of the range of our instrument.

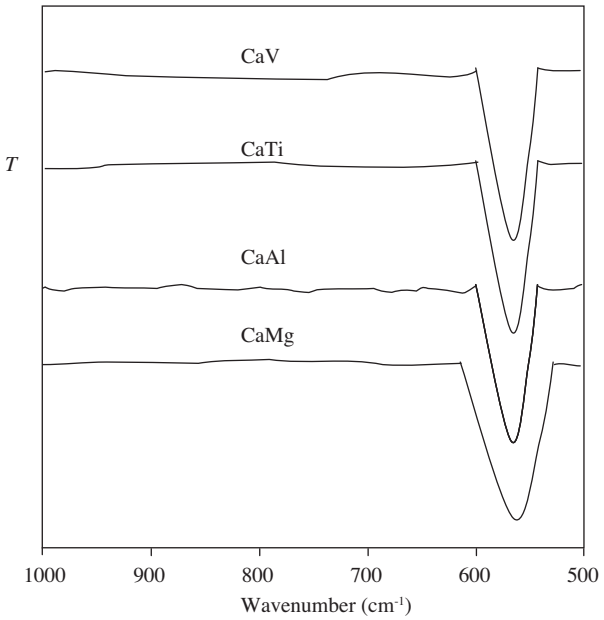

Figure 2. The FTIR spectra of the compounds. The T scale is arbitrary.

Table 2. Magnetic parameters of the studied compounds.

	M_r (emu/g)	H_c (Oe)	T_N (°C)
CaMg	4.5×10^{-2}	89	342
CaAl	8.7×10^{-3}	444	346
CaTi	1.2×10^{-2}	445	349
CaV	1.4×10^{-2}	538	345

The room temperature magnetic hysteresis loops of the studied compounds are shown in Figures 3(a–d). It is clear that all compounds show weak ferromagnetism with no saturation magnetization, with significant loop opening for CaAl, CaTi, and CaV, which confirms the original antiferromagnetic character of the compounds. The deduced values of remnant magnetization M_r and coercivity H_c are listed in Table 2. In general, except for CaTi and CaV, which have nearly the same M_r values, it is seen from the table that there is a fair correspondence between the c/a and M_r values (CaMg has the greatest M_r and c/a values, whereas CaAl has the lowest M_r and c/a values). This means that lattice distortion could be responsible for the variation of the magnetic properties upon substitution. The substitution process will change drastically the bond angle of Fe^{3+}-O^{2-}-Fe^{3+} and distort the FeO_6 octahedra, which results in partial destruction of the spatially modulated spiral spin structure and hence the appearance of weak ferromagnetism in these compounds. Moreover, each compound has a M_r value greater than that of $Bi_{0.9}Ca_{0.1}FeO_3$, studied in our previous work [18], which

suggests that the substitution-induced magnetization is structural in cause, not magnetic. In CaTi and CaV, we expect the magnetization behavior to be a balance between two competing effects: lattice distortion and decrease of the oxygen vacancies resulting from the substitution of the heterovalent ions Ti^{4+} and V^{5+}, so that the compound eventually achieves charge neutrality.

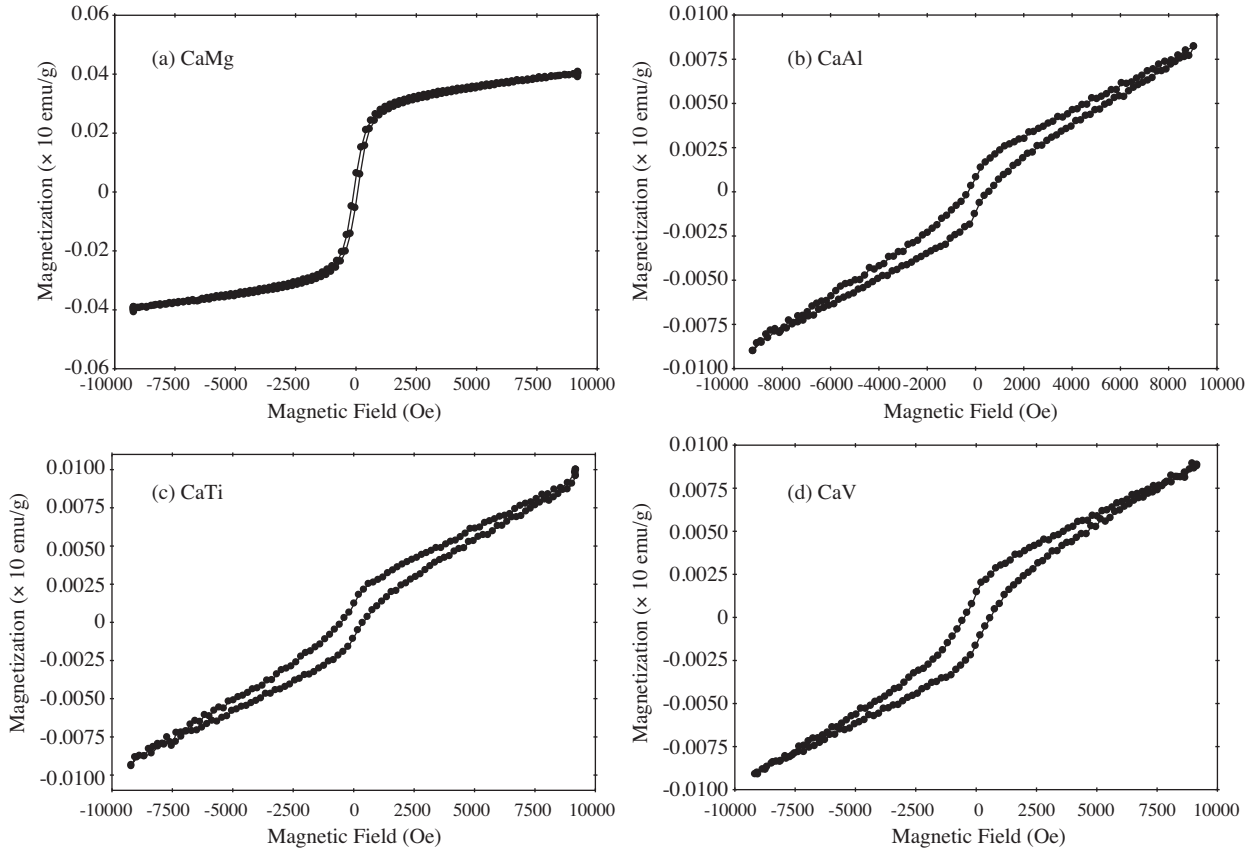

Figure 3. The magnetic hysteresis loops of (a) $Bi_{0.9}Ca_{0.1}Fe_{0.98}Mg_{0.02}O_3$ (labeled as CaMg), (b) $Bi_{0.9}Ca_{0.1}Fe_{0.98}Al_{0.02}O_3$ (CaAl), (c) $Bi_{0.9}Ca_{0.1}Fe_{0.98}Ti_{0.02}O_3$ (CaTi), and (d) $Bi_{0.9}Ca_{0.1}Fe_{0.98}V_{0.02}O_3$ (CaV).

In general, as can be seen from Table 2, the H_c value increases as the valence state of the substituting ion is increased. The increase of H_c may be attributed to the increase of the structural defects [27], which are associated with the substitution process.

It is known that the magnetic transition temperature can be determined by various kinds of measurements such as magnetic susceptibility and thermal expansion coefficient [28]. One reliable method for the determination of the magnetic transition temperature is differential scanning calorimetry (DSC). On a DSC scan, the transition is marked by a weak endothermic peak. However, one has to be careful because such a transition could be masked by other noisy signals. The DSC curves of the studied compounds are shown in Figure 4, drawn after the subtraction of the fluctuating baseline for clarification. The transitions revealed by these curves are magnetic transitions from antiferromagnetic to paramagnetic. As shown in Table 2, the value of the magnetic transition temperature T_N is little affected by the substituting ion type due to its low content. Comparatively, a T_N value of 370 °C was reported for the compounds $BiFe_{0.95}Mn_{0.05}O_3$ [14] and $Bi_{0.85}La_{0.1}Ho_{0.5}FeO_3$ [24], 366 °C for $Bi_{0.9}Tb_{0.1}FeO_3$ [9], and 386 °C for $Bi_{0.8}La_{0.2}FeO_3$ [10], all determined by thermal analysis. It

is obvious that these values (in addition to our cited values) are fluctuating around the well-established value of 370 °C measured for pure BFO. The reason for this fluctuation is that the magnetic transition temperature is dependent on factors such as the type of substituting ions, substitution concentration, preparation method, particle size, and impurity phases.

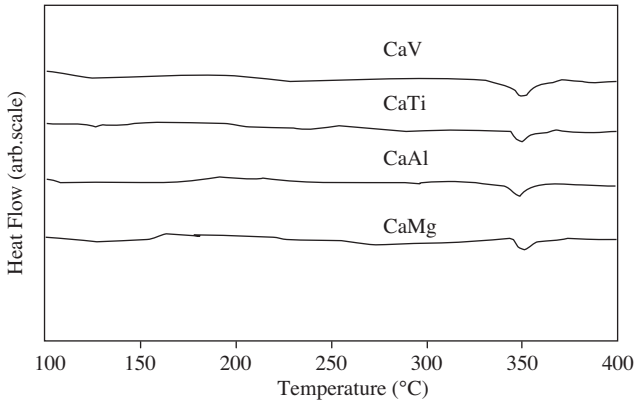

Figure 4. The DSC curves of the compounds.

4. Conclusions

The compounds CaMg, CaAl, CaTi, and CaV were found to have the rhombohedral perovskite-like structure, accompanied by the existence of small amounts of $Bi_2Fe_4O_9$ and $Bi_{25}FeO_{40}$ impurity phases. The FTIR spectra revealed the mode characteristic of Fe-O stretching vibrations. The appearance of weak ferromagnetism in all compounds is believed to arise from partial destruction of the spiral spin structure due to lattice distortion and decrease of oxygen vacancies. The magnetic transition temperatures of the compounds are less than the BFO value by about 20 °C.

References

[1] G. Catalan and J. Scott, *Adv. Mater.,* **21**, (2009), 2463.

[2] S. Pradhan and B. Roul, *J. Phys. Chem. Solids*, **72**, (2011), 1180.

[3] V. Khomchenko, L. Pereira and J. Paixão, *J. Phys. D: Appl. Phys.*, **44**, (2011), 185406.

[4] G. Le Bras, P. Bonville, D. Colson, A. Forget, N. Genand-Riondet and R. Tourbot, *Physica B*, **406**, (2011), 1492.

[5] R. Rai, S. Mishra, N. Singh, S. Sharma and A. Kholkin, *Current Appl. Phys.*, **11**, (2011), 508.

[6] S. Pradhan, J. Das, P. Rout, S. Das, S. Samantray, D. Mishra, D. Sahu, A. Pradhan, K. Zhang, V. Srinivasu and B. Roul, *J. Alloys Compd.*, **509**, (2011), 2645.

[7] N. Minh and N. Quan, *J. Alloys Compd.*, **509**, (2011), 2663.

[8] V. Khomchenko, I. Troyanchuk, M. Bushinsky, O. Mantytskaya, V. Sikolenko and J. Paixão, *Mater. Lett.*, **65**, (2011), 1970.

[9] S. Saxin and C. Knee, *J. Solid State Chem.*, **184**, (2011), 1576.

[10] K. Sen, S. Thakur, K. Singh, A. Gautam and M. Singh, *Mater. Lett.*, **65**, (2011), 1963.

[11] A. Moure, J. Tartaj and C. Moure, *J. Alloys Compd.*, **509**, (2011), 7042.

[12] M. Bernardo, T. Jardiel, M. Peiteado, A. Caballero and M. Villegas, *J. Alloys Compd.*, **509**, (2011), 7290.

[13] Q. Xu, S. Zhou, Z. Wen, D. Wu, T. Qiu, M. Xu, K. Potzger and H. Schmidt, *Phys. Lett.* A, **375**, (2011), 1209.

[14] S. Basu, SK. Hossain, D. Chakravorty and M. Pal, *Current Appl. Phys.*, **11**, (2011), 976.

[15] A. Azam, A. Jawad, A. Ahmed, M. Chaman and A. Naqvi, *J. Alloys Compd.*, **509**, (2011), 2909.

[16] D. Karpinsky, I. Troyanchuk, J. Vidal, N. Sobolev and A. Kholkin, *Solid State Commu.*, **151**, (2011), 536.

[17] C. Shi, X. Liu, Y. Hao and Z. Hu, *Mater. Res. Bull.*, **46**, (2011), 378.

[18] M. Al-Haj, *Cryst Res. Technol.*, **45**, (2010), 89.

[19] B. Luo, C. Chen and K. Jin, *Solid State Commu.*, **151**, (2011), 712.

[20] A. Kumar and K. Yadav, *Mat. Sci. Eng. B*, **176**, (2011), 227.

[21] J. Yang, X. Li, J. Zhou, Y. Tang, Y. Zhang and Y. Li, *J. Alloys Compd.*, **509**, (2011), 9271.

[22] A. Gautam, K. Singh, K. Sen, R. Kotnala and M. Singh, *Mater. Lett.*, **65**, (2011), 591.

[23] X. Chen, Z. Qiu, J. Zhou, G. Zhu, X. Bian and P. Liu, *Mater. Chem. Phys.*, **126**, (2011), 560.

[24] X. Zhang, Y. Sui, X. Wang, J. Mao, R. Zhu, Y. Wang, Z. Wang, Y. Liu and W. Liu, *J. Alloys Comp.*, **509**, (2011), 5908.

[25] M. Al-Haj, *Cryst. Res. Technol.*, **45**, (2010), 1145.

[26] R. Shannon, *Acta Crystallogr. A*, **32**, (1976), 751.

[27] W. Callister and D. Rethwisch, Materials science and engineering, 8^{th} edition, (Wiley, Chichester, 2011) p. 820.

[28] C. Kittel, Introduction to solid state physics, 8^{th} edition, (Wiley, Chichester, 2005) p. 342.